Surface Chemistry

DOI: 10.1002/ange.201201349

Surface Science Approach to the Solid–Liquid Interface: Surface-Dependent Precipitation of $Ni(OH)_2$ on α-Al_2O_3 Surfaces**

*Asma Tougerti, Isabelle Llorens, Francesco D'Acapito, Emiliano Fonda, Jean-Louis Hazemann, Yves Joly, Dominique Thiaudière, Michel Che, and Xavier Carrier**

A molecular-scale understanding of the adsorption of metal ions on oxide surfaces is of fundamental importance for various scientific areas where the oxide/water interface plays a central role, such as corrosion science, preparation of heterogeneous catalysts, transport of contaminants in the environment. As a matter of fact, a fine-tuning of metal speciation during the first steps of heterogeneous catalyst preparation (oxide/water interface) will strongly control the final characteristics of the catalyst (activity/selectivity/stability).[1] However, a rational description of sorption mechanisms is generally made difficult by the ill-defined surface structure of high surface area oxides exposing a number of different sorption sites.[2] One way to mitigate this problem is to simplify the sorption system by using oriented single crystals that have a limited number of well-defined surface sites. This reductionist approach applied to aqueous deposition is almost inexistent in the field of surface science where most of the model studies use nonaqueous deposition techniques such as metal evaporation.[3] However, pioneering works of the research groups of Brown, Jr.[4] in the field of earth sciences and Niemantsverdriet,[5] Regalbuto,[6] or more recently Freund[7] in the field of catalysis have shown the tremendous importance of developing a surface science approach using a realistic aqueous phase deposition method.

Aqueous deposition of Ni^{II} complexes on α-Al_2O_3 single crystals has been chosen in this work since this system has practical implications in heterogeneous catalysis for hydrotreating (removal of S, N, O, and metals from crude oil in refineries), hydrogenation, or steam reforming purposes.[8] α-Al_2O_3 single crystals are commercially available in two orientations, (0001) and $(1\bar{1}02)$, exposing different types of surface sites partly mimicking the complexity of the surface chemistry of γ-Al_2O_3, the standard catalytic support, that is not available as single crystals.[9] Moreover, both (0001) and $(1\bar{1}02)$ α-Al_2O_3 orientations have been extensively characterized in the presence of water.[10] However, the use of single crystals with low surface area requires characterization of very low quantities of adsorbates. Hence, grazing-incidence X-ray absorption spectroscopy (GI-XAS) was chosen as the main molecular-scale characterization technique, since detection of a small amount of adsorbates is made possible by enhancement of the fluorescence intensity in the grazing-incidence geometry.[11]

Furthermore, the combined use of GI-XAS and oriented single crystals provide additional structural information on the local environment of the absorbing atom thanks to the synchrotron beam polarization. Actually, the measured number of neighbors ($N_{measured}$) will be three times higher than the actual number of neighbors (N_{real}) when the chemical bond (directed along $\vec{r}$) is parallel to the electric field vector $\vec{\varepsilon}$ [Eq. (1), $\cos\theta = 1$].[12]

$$N_{measured}(\theta) = \sum_{i=1}^{N_{real}} 3[\vec{\varepsilon}, \vec{r}]^2 = 3\sum_{i=1}^{N_{real}} cos^2\theta \qquad (1)$$

Ni^{II} adsorption on (0001) and $(1\bar{1}02)$ α-Al_2O_3 single-crystal surfaces was studied in the presence of ethylenediamine (en, that is, $NH_2(CH_2)_2NH_2$) to investigate the effect of classical chelating ligands in improving the Ni dispersion in alumina-supported Ni catalysts.[13] Al_2O_3-supported model catalysts were thus prepared by aqueous phase deposition of Ni^{II} on 2″-diameter α-Al_2O_3 single-crystal wafers (from Saint-Gobain Crystals) with two orientations: (0001) and $(1\bar{1}02)$. Ni adsorption was performed by equilibrating the α-Al_2O_3 wafers in a $Ni(NO_3)_2$ solution with a en to Ni ratio of 1. The samples will be designated $Ni(en)_1/(1\bar{1}02)$ or (0001) depending on the single-crystal orientation. In the impregnation conditions, both surfaces are fully hydroxylated as shown by the XPS signature of surface OH (binding energy 532.4 eV, see section S1a in the Supporting Information). Furthermore, XPS shows that the hydroxyl content on both surfaces is comparable with similar surface OH density: 10.3 at nm^{-2} for (0001) and 13.3 at nm^{-2} for $(1\bar{1}02)$.

Ni sorption experiments revealed that the (0001) α-Al_2O_3 surface is absolutely inert since XPS results did not show any

[*] Dr. A. Tougerti, Prof. M. Che, Prof. X. Carrier
UPMC-Université Pierre et Marie Curie
Laboratoire de Réactivité de Surface
75252 Paris Cedex 05 (France)
E-mail: xavier.carrier@upmc.fr
Dr. I. Llorens
CEA/DSM/INAC/CNRS, Grenoble (France)
Dr. F. D'Acapito
ESRF-GILDA, Grenoble (France)
Dr. E. Fonda, Dr. D. Thiaudière
Synchrotron Soleil, Gif-sur-Yvette (France)
Dr. I. Llorens, Dr. J.-L. Hazemann
ESRF-FAME, Grenoble (France)
Dr. J.-L. Hazemann, Dr. Y. Joly
Institut Néel, CNRS-Université J. Fourier Grenoble (France)

[**] We thank Drs. Y. Hou, J. Blanchard, L. Stievano, and O. Proux for help with the XAS experiments, Dr. C. Methivier for assistance in XPS analysis and Dr. V. Humblot for support with the AFM data collection. We are also grateful to the beamline staffs at ESRF (GILDA and FAME) and SOLEIL (DIFFABS and SAMBA) for their valuable assistance.

Supporting information for this article is available on the WWW under http://dx.doi.org/10.1002/anie.201201349.

© 2012 Wiley-VCH Verlag GmbH & Co. KGaA, Weinheim

Ni uptake for Ni(en)$_1$/(0001) in our experimental conditions. Changing the experimental parameters (baking the crystal at lower temperature, modifying the solution pH and/or increasing the wafer/Ni–solution contact time) did not increase the Ni uptake.

Conversely, Ni adsorption on the (1$\bar{1}$02) α-Al_2O_3 orientation is shown by XPS (see section S1b in the Supporting Information) since a Nickel surface density of 9.4 at nm^{-2} can be determined following equation (1) in Towle et al.[14] Yet, this amount is probably underestimated if a surface precipitate is formed as shown below.[15] Figure 1 shows GI-EXAFS

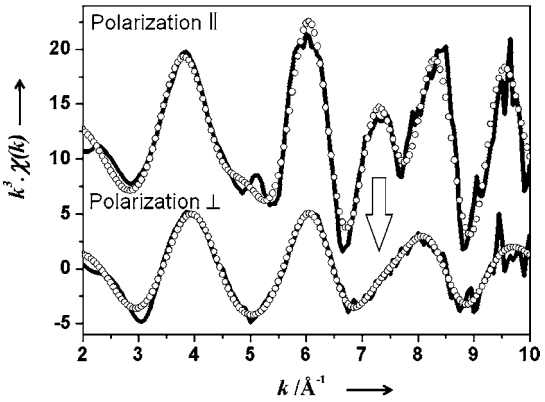

Figure 1. k^3-weighted Ni K-edge EXAFS spectra (full line) and corresponding fit (dotted line) for Ni(en)$_1$/(1$\bar{1}$02) dried at room-temperature for parallel and perpendicular polarizations.

(EXAFS = extended X-ray absorption fine structure) spectra obtained for Ni(en)$_1$/(1$\bar{1}$02) dried at room temperature for the parallel and perpendicular polarizations. The dissimilarity of both spectra clearly indicates a polarization effect. For the parallel polarization, a beat pattern at (7–8) Å^{-1} suggests a contribution of various shells of atoms. This beat pattern is characteristic of α-Ni(OH)$_2$ and the absence of a double oscillation at 8.0 and 8.5 Å^{-1} rules out the presence of Al-containing layered double hydroxides (hydrotalcites) identified in other systems.[16] On the other hand, the EXAFS spectrum for the parallel polarization can be described as a single oscillation arising from a single type of neighbor.

This polarization dependence is confirmed by examination of the Fourier Transforms obtained from the EXAFS signals (Figure 2). As a matter of fact, the second peak (apparent distance of 2.7 Å) is much more intense for the parallel polarization. This polarization effect is also clearly demonstrated by fitting the EXAFS spectra (see section S2 in the Supporting Information) with Ni-O and Ni-Ni paths. The parallel polarization is well fitted with six O neighbors at 2.02 Å and six Ni atoms at 3.08 Å while the coordination numbers are clearly lower for the perpendicular polarization with 4.1 O atoms and 0.8 Ni atoms at 2.04 and 3.15 Å, respectively. The Ni–O and Ni–Ni distances for the parallel polarization are in good agreement with those of Ni(OH)$_2$[16] strongly suggesting surface precipitation of nickel hydroxide on the (1$\bar{1}$02) α-alumina surface. Moreover, nitrogen was not detected with XPS discarding a simple adsorption of Ni(en)$_1$

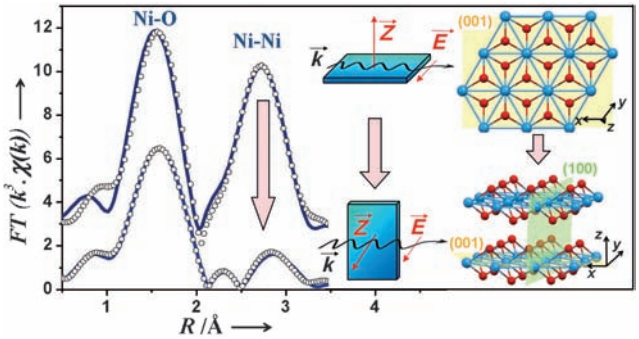

Figure 2. Fourier transforms (Δk = 3.3–9.9 Å^{-1}) of k^3-weighted Ni K-edge EXAFS spectra (uncorrected for phase-shift) obtained for parallel (top) and perpendicular (bottom) polarizations and the corresponding fits (dotted line) for Ni(en)$_1$/(1$\bar{1}$02). The Ni(OH)$_2$ structure is also given with a single layer (top, (001) orientation) and two stacked layers in the [001] direction (bottom). Ni atoms are in blue and oxygen atoms in red. $\vec{k}$ is the wave vector, $\vec{Z}$ is the normal vector, and $\vec{E}$ is the electric field vector.

(see section S1c in the Supporting Information). The strong reduction in the apparent Ni-Ni coordination numbers for the perpendicular polarization can be explained by a surface-induced oriented precipitation of Ni(OH)$_2$ parallel to the (1$\bar{1}$02) surface. As a matter of fact, Ni(OH)$_2$ adopts a brucite-type structure with Ni(OH)$_2$ layers stacked along the [001] axis (Figures 2 and 3).[17] If one considers an oriented precipitation of Ni(OH)$_2$ with its [001] axis perpendicular to

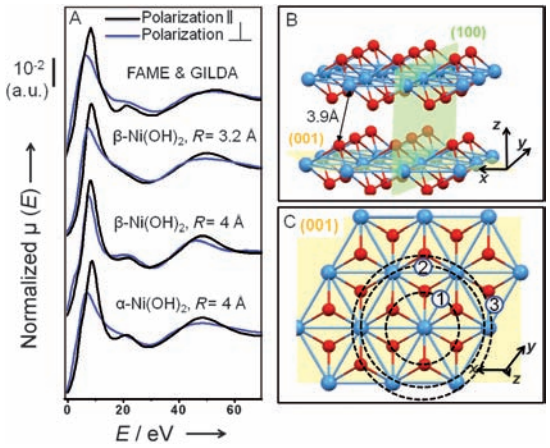

Figure 3. A) Experimental Ni K-edge XANES spectra for Ni(en)$_1$/(1$\bar{1}$02) for parallel and perpendicular polarization directions and comparison to FDMNES calculations for both polarization directions and different cluster radii (R). B) Representation of the structure of Ni(OH)$_2$ along the z axis (red atoms: oxygen, blue atoms: nickel). C) Representation of the (001) plane of Ni(OH)$_2$. The numbers indicate the different shells with respect to the central Ni atom.

the α-alumina surface, GI-EXAFS spectroscopy with a parallel polarization will probe Ni-Ni pairs in the (001) plane with six Ni second neighbors (Figure 2). Following this hypothesis, the apparent number of Ni neighbors at about 3.1 Å should be zero for the perpendicular polarization since there are no Ni

© 2012 Wiley-VCH Verlag GmbH & Co. KGaA, Weinheim

second neighbors in the direction perpendicular to the (001) plane. A slightly higher Ni-Ni coordination number of 0.8 is found that may be explained either by adsorption of a small amount of polymeric Ni species with a low cluster size or by the presence of a weak fraction of $Ni(OH)_2$ that precipitates in a nonoriented way.

The polarization dependence observed in EXAFS is further demonstrated by examination of the X-ray absorption near-edge structure (XANES) region for both perpendicular and parallel polarizations (Figure 3). The main differences between both polarizations lie 1) in the white line intensity and 2) in a shoulder at about 15 eV above the edge better resolved and more intense for the parallel polarization. To confirm that these differences can be explained by a surface-induced oriented precipitation of $Ni(OH)_2$, XANES calculations for $Ni(OH)_2$ oriented along the [001] and [100] crystal directions were performed using ab initio simulations with the FDMNES package (Figure 3).[18]

A cluster size of 3.2 Å radius (including the 1st oxygen shell and the 2nd Ni shell) is too small for reproducing the experimental spectral features of the parallel polarization (Figure 3, β-$Ni(OH)_2$, $R = 3{,}2$ Å). However, when increasing the cluster size to 4 Å, and thus including both the third oxygen shell in the (001) plane (Figure 3C) and the oxygen atoms located in the parallel layer (Figure 3B), an accurate reproduction of the parallel experimental spectrum is obtained (Figure 3, β-$Ni(OH)_2$, $R = 4$ Å). Yet, the calculated spectra are independent of the polarization in contradiction with the experimental results. This apparent contradiction can be explained by considering that the oxygen atoms located in the parallel layer are not contributing to the XANES signal for the perpendicular polarization because either the interlamellar distance in the $Ni(OH)_2$ precipitate is longer than 4 Å or a single layer of $Ni(OH)_2$ is formed. This last hypothesis can be ruled out with the help of AFM (see section S3 in the Supporting Information) since a topographic analysis of the surface for $Ni(en)_1/(1\bar{1}02)$ shows that the precipitate has a thickness of at least 15 Å. The first hypothesis (interlamellar distance higher than 4 Å) is thus more probable and suggests the precipitation of the α-$Ni(OH)_2$ polymorph on the $(1\bar{1}02)$ α-Al_2O_3 surface rather than the β form since the main difference between both $Ni(OH)_2$ polymorphs lies in the interlamellar distance. For the β form, layers are perfectly stacked and separated by 4.6 Å[17] while for the α form, the interlamellar distance is much larger (7.6 Å), with $Ni(OH)_2$ layers randomly oriented (turbostratic structure).[19] The preferential precipitation of α-$Ni(OH)_2$ was confirmed by calculating its theoretical XANES spectrum (Figure 3, α-$Ni(OH)_2$, $R = 4$ Å) which is in good agreement with the experimental spectrum.

Precipitation of α-$Ni(OH)_2$ has already been reported for Si-containing powder oxides such as talc and silica while surface deposition of Ni–Al layered double hydroxides (LDH) was reported for Al-containing supports (pyrophyllite, gibbsite, and γ-Al_2O_3).[16] Yet, careful examination of EXAFS oscillations (Figure 1) allowed us to exclude LDH formation in our conditions. The very low solubility of α-Al_2O_3, the negligible surface area of planar wafers as well as the Ni-complexing ability of ethylenediamine can explain that α-$Ni(OH)_2$ precipitation is favored over LDH formation as observed previously by Yamaguchi et al.[20]

Our results demonstrate that the surface does not play the simple role of physical container since the type of alumina surface sites does play a crucial role for the formation and orientation of the surface Ni hydroxide. As a matter of fact, neither adsorption nor precipitation of Ni is observed on the (0001) surface. The lack of Ni^{II} adsorption can be related to the absence of surface charge since surface OH groups on the (0001) face (Al_{6C}-μ_2-OH)[21] are neutral over most of the pH range[22] and will consequently not favor cationic complexes adsorption. The neutrality of the surface most probably explains the absence of reactivity of the (0001) orientation.

Conversely, our results demonstrate that the $(1\bar{1}02)$ α-alumina surface promotes $Ni(OH)_2$ precipitation. Surface precipitation is further established by the surface-induced orientation of the α-$Ni(OH)_2$ precipitate. Surface precipitation can encompass different meanings since it can have a thermodynamic origin (precipitation for concentrations that are undersaturated with respect to homogeneous precipitation)[15,20,23] or a kinetic origin (exclusive precipitation on the surface, heterogeneous precipitation, for supersaturated solutions). In our conditions, it is not straightforward to discriminate both phenomena since it depends on the saturation of the solution. Actually, examination of the solubility diagram (see section S4 in the Supporting Information) shows that the Ni solution (0.5 M) is just at the saturation limit with respect to $Ni(OH)_2$ precipitation at our impregnation pH (i.e. 7) with a en/Ni ratio of 1. However it cannot be irrefutably concluded on the saturation of the solution since 1) there is a large uncertainty in the solubility constants, 2) EXAFS identified the precipitate to be α-$Ni(OH)_2$ which should be more soluble than the thermodynamically stable phase β-$Ni(OH)_2$ considered in solubility studies and 3) no precipitate was formed in homogeneous solution after long ageing times. However the adsorption isotherm obtained for lower Ni concentrations (see section S5 in the Supporting Information) shows a marked increase in adsorption at 0.05 M, that is, well below the solubility of $Ni(OH)_2$. Moreover, above this concentration, XPS analysis indicates the absence of N on the surface (as for the 0.5 M concentration) confirming that Ni sorption is not a simple site adsorption of $Ni(en)_1$ but proceeds through a surface-induced precipitation in conditions that are undersaturated with respect to the solubility of $Ni(OH)_2$. The concept of surface precipitation has been thoroughly discussed by Towle et al.[15] using thermodynamic reasoning. One important conclusion is that changes in the properties of the solution in the vicinity of the surface cannot induce precipitation. The only explanation able to rationalize surface precipitation in the case of undersaturated solutions is to consider that there is a reduction in the free-energy of the solid phase. Minimization of the surface energy between the alumina surface and the α-$Ni(OH)_2$ precipitate could give a rational explanation for the surface-oriented precipitation of the latter.

Whatever the origin of the observed surface-induced precipitation (be it thermodynamic or kinetic), the exclusive surface precipitation has to be initiated by nuclei formation induced by grafting of $[Ni(en)(H_2O)_4]^{2+}$ on the Al_2O_3 surface

 © 2012 Wiley-VCH Verlag GmbH & Co. KGaA, Weinheim

as previously demonstrated on powders.[13] As a matter of fact, adsorption and precipitation are closely interconnected as shown previously on carbon nanofibers by van der Lee et al.[24] The inertness of the (0001) orientation is then related to the lower basicity of doubly coordinated surface OH groups (Al_{6C}-μ_2-OH) with respect to tetrahedrally coordinated surface OH (Al_{4C}-μ_1-OH) exposed on the $(1\bar{1}02)$ α-alumina surface[10a] that are prone to substitute aqua ligands in the Ni coordination sphere.

In conclusion, the surface science approach used in this work combined with an aqueous phase deposition method shows a surface-dependent and oriented precipitation of α-$Ni(OH)_2$ during Ni^{II} deposition on α-Al_2O_3 single-crystal surfaces. Polarization-dependent EXAFS, in good agreement with XANES ab initio simulations, proves that the surface precipitate is oriented parallel to the $(1\bar{1}02)$ face while no deposition of Ni^{II} takes place on the (0001) surface. Surface precipitation can be explained by surface grafting of the Ni precursor ($[Ni(en)(H_2O)_4]^{2+}$) exclusively on the $(1\bar{1}02)$ α-Al_2O_3 face and minimization of the total surface energy between the Al_2O_3 surface and α-$Ni(OH)_2$.

These results suggest that Ni dispersion on powdered Al_2O_3 is highly heterogeneous on individual oxide particles depending on exposed surfaces and thus on the morphology of the particles. The use of planar model systems emphasizes the crucial role of specific Al_2O_3 surface orientations for controlling Ni adsorption and dispersion in industrially relevant catalysts.

Experimental Section

Prior to Ni adsorption, α-Al_2O_3 single crystals were cleaned by successive washing with Milli-Q water (resistivity 18.2 MΩ cm, total organic carbon, TOC, < 5 ppb) HNO_3, NH_3 and again Milli-Q water before calcination overnight in air at 700 °C. Ni adsorption was performed by equilibrating the α-Al_2O_3 wafers 5 h in 25 mL of a 0.5 M $Ni(NO_3)_2$ (99.999% purity) solution containing one equivalent of ethylenediamine (en, 99.5% purity) per Ni (en/Ni = 1). The pH of the adsorption solution was 7. In these conditions, the Ni speciation diagram in solution shows that 60% of the Ni species are $[Ni(en)(H_2O)_4]^{2+}$, 30% are $[Ni(en)_2(H_2O)_2]^{2+}$, and 10% are $[Ni(H_2O)_6]^{2+}$ (see section S6 in the Supporting Information). The wafers were then withdrawn from the solution after 5 h of equilibration and washed with Milli-Q water before drying at room-temperature in a flow of nitrogen.

Characterization was performed with GI-EXAFS spectroscopy at the Ni K edge (8333 eV) on four different beamlines: CRG-FAME (BM30B)[25] and GILDA (BM08) [26] at the ESRF (Grenoble, France) and DIFFABS and SAMBA[27] at SOLEIL (Gif-sur-Yvette, France) to change the orientation of the wafer with respect to the polarization of the synchrotron beam. A first set of experiments was conducted on FAME and GILDA with a single polarization on each beamline and a second set of experiments was later conducted on DIFFABS and SAMBA using both polarizations to ensure the reproducibility of the adsorption experiments and the observed polarization effect (see section S7 in the Supporting Information). The electric-field vector of the synchrotron beam was respectively perpendicular and parallel to the wafer surface for the FAME and GILDA beamlines (Figure 2). XANES spectra were also calculated by ab initio simulations using the FDMNES package.[18]

Received: February 17, 2012
Revised: June 1, 2012
Published online: June 22, 2012

Keywords: alumina · surface chemistry · X-ray absorption spectroscopy

[1] E. Marceau, X. Carrier, M. Che, O. Clause, C. Marcilly in *Handbook of Heterogeneous Catalysis* (Eds.: G. Ertl, H. Knözinger, F. Schüth, J. Weitkamp), Wiley-VCH, Weinheim, **2008**, pp. 467 – 484.
[2] G. E. Brown, Jr., V. E. Henrich, W. H. Casey, D. L. Clark, C. Eggleston, A. Felmy, D. W. Goodman, M. Grätzel, G. Maciel, M. I. McCarthy, K. Nealson, D. A. Sverjensky, M. F. Toney, J. M. Zachara, *Chem. Rev.* **1999**, *99*, 77 – 174.
[3] M. Heemeier, S. Stempel, S. K. Shaikhutdinov, J. Libuda, M. Bäumer, R. J. Oldman, S. D. Jackson, H. J. Freund, *Surf. Sci.* **2003**, *523*, 103 – 110.
[4] J. R. Bargar, S. N. Towle, G. E. Brown, Jr., G. A. Parks, *J. Colloid Interface Sci.* **1997**, *185*, 473 – 492.
[5] G. Kishan, J. A. R. van Veen, J. W. Niemantsverdriet, *Top. Catal.* **2004**, *29*, 103 – 110.
[6] C. Park, P. A. Fenter, N. C. Sturchio, J. R. Regalbuto, *Phys. Rev. Lett.* **2005**, *94*, 076104.
[7] H.-F. Wang, H. Ariga, R. Dowler, M. Sterrer, H.-J. Freund, *J. Catal.* **2012**, *286*, 1 – 5.
[8] a) J. Kibsgaard, A. Tuxen, K. G. Knudsen, M. Brorson, H. Topsøe, E. Lægsgaard, J. V. Lauritsen, F. Besenbacher, *J. Catal.* **2010**, *272*, 195 – 203; b) J. Sehested, *Catal. Today* **2006**, *111*, 103 – 110.
[9] P. Euzen, P. Raybaud, X. Krokidis, H. Toulhoat, J. L. Le Loarer, J. P. Jolivet, C. Froidefond in *Handbook of Porous Solids*, *Vol. 3* (Eds.: F. Schüth, K. S. W. Sing, J. Weitkamp), Wiley-VCH, Weinheim, **2002**, pp. 1591 – 1677.
[10] a) A. Tougerti, C. Methivier, S. Cristol, F. Tielens, M. Che, X. Carrier, *Phys. Chem. Chem. Phys.* **2011**, *13*, 6531 – 6543; b) T. P. Trainor, P. J. Eng, G. E. Brown, Jr., I. K. Robinson, M. D. Santis, *Surf. Sci.* **2002**, *496*, 238 – 250.
[11] S. M. Heald, E. Keller, E. A. Stern, *Phys. Lett. A* **1984**, *103*, 155 – 158.
[12] M. Shirai, T. Inoue, H. Onishi, K. Asakura, Y. Iwasawa, *J. Catal.* **1994**, *145*, 159 – 165.
[13] F. Négrier, E. Marceau, M. Che, J.-M. Giraudon, L. Gengembre, A. Löfberg, *J. Phys. Chem. B* **2005**, *109*, 2836 – 2845.
[14] S. N. Towle, J. R. Bargar, G. E. BrownJr, G. A. Parks, *J. Colloid Interface Sci.* **1999**, *217*, 312 – 321.
[15] S. N. Towle, J. R. Bargar, G. E. BrownJr, G. A. Parks, *J. Colloid Interface Sci.* **1997**, *187*, 62 – 82.
[16] A. C. Scheinost, D. L. Sparks, *J. Colloid Interface Sci.* **2000**, *223*, 167 – 178.
[17] R. W. G. Wyckoff, *Crystal Structures*, Interscience, New York, **1964**.
[18] Y. Joly, *Phys. Rev. B* **2001**, *63*, 125120 – 125129.
[19] S. Le Bihan, M. Figlarz, *J. Cryst. Growth* **1972**, *13 – 14*, 458 – 461.
[20] N. U. Yamaguchi, A. C. Scheinost, D. L. Sparks, *Soil Sci. Soc. Am. J.* **2001**, *65*, 729 – 736.
[21] P. J. Eng, T. P. Trainor, G. E. Brown Jr., G. A. Waychunas, M. Newville, S. R. Sutton, M. L. Rivers, *Science* **2000**, *288*, 1029 – 1033.
[22] J. P. Fitts, X. Shang, G. W. Flynn, T. F. Heinz, K. B. Eisenthal, *J. Phys. Chem. B* **2005**, ASAP.
[23] K. J. Farley, D. A. Dzombak, F. M. M. Morel, *J. Colloid Interface Sci.* **1985**, *106*, 226 – 242.

 © 2012 Wiley-VCH Verlag GmbH & Co. KGaA, Weinheim

[24] M. K. van der Lee, J. van Dillen, J. H. Bitter, K. P. de Jong, *J. Am. Chem. Soc.* **2005**, *127*, 13573 – 13582.
[25] O. Proux, X. Biquard, E. Lahera, J. J. Menthonnex, A. Prat, O. Ulrich, Y. Soldo, P. Trévisson, G. Kapoujyan, G. Perroux, P. Taunier, D. Grand, P. Jeantet, M. Deleglise, J. P. Roux, J. L. Hazemann, *Phys. Scr.* **2005**, *T115*, 970 – 973.
[26] F. D'Acapito, I. Davoli, P. Ghigna, S. Mobilio, *J. Synchrotron Radiat.* **2003**, *10*, 260 – 264.
[27] F. Baudelet, R. Belkhou, V. Briois, A. Coati, P. Dumas, V. H. Etgens, A.-M. Flank, P. Fontaine, Y. Garreau, O. Lyon, I. Quinkal, F. Rochet, P. Roy, M. Sauvage, F. Sirotti, A. Somogyi, D. Thiaudière, *Oil Gas Sci. Technol.* **2005**, *60*, 849 – 874.

 © 2012 Wiley-VCH Verlag GmbH & Co. KGaA, Weinheim